excludes the presence of the hydroxo species, is similar to that of the solid complex. The susceptibility lowers significantly on increasing the pH and the hydroxo species concentration. In conclusions, the formation of the monohydroxo species, its high formation constant, and its influence on the magnetic susceptibility are experimental evidence that make reasonable the hypothesis that this species has the hydroxide ion bridging the two metal ions with consequent increasing of the metal–metal interaction.

Electrochemical Studies. An aqueous solution of the $[Cu_2(bristrien)]^{4+}$ complex has been investigated by using the CV technique. At a potential scan rate of 200 mV s^{-1} for higher the current/potential profile shows two consecutive peaks in reduction, followed, in the reversed scan, by two oxidation peaks (see Figure 4). The separation between the peaks, more evident in the reduction scan, is about 150 mV. The peaks do not shift on the potential axis as a function of scan rate. The intensity of each peak, in comparison with a monoelectronic standard (e.g., $[Ni(cyclam)](ClO_4)_2$[35]) would correspond to the addition of 1 e. Thus, the dinuclear species $[Cu_2(bistrien)]^{4+}$ presents a behavior corresponding to a two-electron reversible reduction into the dinuclear Cu(I) species, by two independent monoelectronic steps. It is worth observing that for a potential scan rate lower than 200 mV s^{-1} an anodic peak appears in the oxidation scan at ca. −145 mV whose intensity increases with the decreasing of the scan rate (see Figure 4). Such a peak should be ascribed to the anodic stripping due to the oxidation of deposited copper metal.[36] In fact, during the controlled-potential electrolysis at the potential of the second peak of reduction (−525 mV), deposition of the copper metal on the surface of the platinum electrode was observed. All this evidence suggests that the $[Cu^I_2(bistrien)]^{2+}$ species is unstable with respect to the disproportionation by which copper metal is produced. Such behavior, already observed in mononuclear complexes of Cu(II) and tetraaza macrocycles,[37] is justified by the instability of the binuclear cuprous species.

Acknowledgment. We thank P. Innocenti for recording NMR spectra and the ISSECC Institute for computing and crystal data collection facilities. Financial support from Progetto Finalizzato Chimica Fine e Secondaria of the Italian Research Council (CNR) is gratefully acknowledged.

Registry No. **1**·8HCl, 94957-30-9; **2**, 94957-31-0; $[Cu_2(bistrien)Cl_2](ClO_4)_2$, 94957-29-6.

Supplementary Material Available: Listings of observed and calculated structure factors, thermal parameters, and hydrogen atom coordinates and a stereoview of the crystal packing of the title compound (11 pages). Ordering information is given on any current masthead page.

(35) Sabatini, L.; Fabbrizzi, L. *Inorg. Chem.* **1979**, *18*, 438.

(36) Zanello, P.; Fabbrizzi, L.; Seeber, R.; Cinquantini, A.; Mazzocchin, G. A. *J. Chem. Soc., Dalton Trans.* **1982**, 893.

(37) Fabbrizzi, L.; Lari, A.; Poggi, A.; Seghi, B. *Inorg. Chem.* **1982**, *21*, 2083.

Contribution from the Departamento de Química Inorgánica, Facultad de Ciencias, Universidad de Málaga, Málaga, Spain 29004

Intercalation of Polar Organic Compounds into $Sn(HPO_4)_2·H_2O$

ENRIQUE RODRÍGUEZ-CASTELLÓN,* AURORA RODRÍGUEZ-GARCIA, and SEBASTIAN BRUQUE

Received May 8, 1984

Several types of amines and amides, and dimethyl sulfoxide, were intercalated in the layered structure of tin(IV) hydrogen phosphate hydrate ($Sn(HPO_4)_2·H_2O$). Pyridine, 4,4′-bipyridine, and dimethyl sulfoxide form a monolayer, while piperidine, aniline, *m*-toluidine, and 3,5-dimethylaniline form a bilayer. The stoichiometry is governed by the "covering effect". A qualitative study of this phenomenon is reported for pyridine. Many quest molecules suitable for layered host structure (urea, thiourea, and formamide) do not intercalate. However, a slightly more basic molecule such as *N*,*N*-dimethylformamide does. The thermal decomposition of the resulting intercalates takes place in three stages: dehydration, removal of the organic molecule, and condensation of the hydrogen phosphate to pyrophosphate.

Introduction

Crystalline tin(IV) hydrogen phosphate (α-SnP) possesses a layered lattice structure similar to that of zirconium(IV) hydrogen phosphate (α-ZrP).[1-3] The metal atoms lie nearly in a plane; they are bridged by phosphate groups. Three oxygens of each phosphate are linked to three tin atoms. Each metal atom is thus octahedrally coordinated by oxygen. The fourth oxygen of each phosphate group bears a proton. The interlayer distance is 7.8 Å.

Very little work has been done on the intercalation chemistry of α-SnP. Michel and Weiss[4] showed that α-SnP undergoes unidimensional swelling when contacted with octylamine, dioctylamine, and trioctylamine. In a previous paper,[5] we reported the formation of complexes between *n*-alkylamines and α-SnP. The intercalation chemistry of layered phosphates has become important as a result of the better understanding of the structure and properties of these compounds.

Experimental Section

Preparation of Tin(IV) Hydrogen Phosphate. To 1 L of 8 M H_3PO_4 and 3 M HNO_3 was added a solution of anhydrous tin(IV) chloride, until the P:Sn ratio was 30. Although the precipitation was complete in 2 days, refluxing was continued for ~150 h. After refluxing, the material was washed with distilled water and then batch treated with 1 M HNO_3 to ensure complete conversion to the H^+ form. The material was again washed with distilled water to a pH of 3.4–4.0, separated by centrifuge, and then air dried.[6,7] The chemical composition was determined by dissolving the phosphate in 1 M NaOH. The phosphate content was determined colorimetrically.[8] Tin(IV) was determined by precipitation with cupferron and calcination to SnO_2.[9] Water was determined by thermogravimetric analysis. Anal. Calcd for $Sn(HPO_4)_2·H_2O$: SnO_2, 45.85; P_2O_5, 43.19; H_2O, 10.96. Found: SnO_2, 46.99; P_2O_5, 41.87; H_2O, 11.29.

(1) Chernorukow, N. G.; Mochalova, I. R.; Moscuichev, E. P.; Sibrina, G. B. *Zh. Prikl. Khim. (Leningrad)* **1977**, *50*, 1618.
(2) Clearfield, A.; Smith, G. D. *Inorg. Chem.* **1969**, *8*, 431.
(3) Troup, J. M.; Clearfield, A. *Inorg. Chem.* **1977**, *16*, 331.
(4) Michel, E.; Weiss, A. *Z. Naturforsch., B: Anorg. Chem. Org. Chem., Biochem., Biophys., Biol.* **1965**, *20B*, 1307.
(5) Rodríguez-Castellón, E.; Bruque, S.; Rodríguez-Garcia, A. *J. Chem. Soc., Dalton Trans.* **1985**, 213.
(6) Costantino, U.; Gasperoni, A. *J. Chromatogr.* **1970**, *51*, 289.
(7) Fuller, M. J. *J. Inorg. Nucl. Chem.* **1971**, *33*, 559.
(8) Alberti, G.; Cardini-Galli, P.; Costantino, U.; Torraca, E. *J. Inorg. Nucl. Chem.* **1967**, *29*, 571.
(9) Heyn, A. H.; Dove, N. G. *Talanta* **1966**, *13*, 33.

0020-1669/85/1324-1187$01.50/0

Table I. Interlayer Distance, Composition, and Methods of Preparation of Intercalation Compounds of α-$Sn(HPO_4)_2 \cdot H_2O$ with Some Polar Organic Compounds

intercalated molecule (IM)	interlayer dist, Å	mol of IM/mol of α-SnP	methods of prepn
pyridine	11.48	0.41	*a, b*
4,4′-bipyridine	12.43	0.25	*b*
piperidine	15.7	1.26	*a*
aniline	19.1	2.0	*a*
m-toluidine	19.2	2.0	*a*
3,5-dimethylaniline	19.5	1.4	*a*
N,N-dimethylformamide	13.3	0.59	*a*
dimethyl sulfoxide	11.4	1.0	*c*

[a] The corresponding pure liquid was allowed to stand with α-SnP for 4 days at 25 °C. [b] A concentrated benzenic solution was allowed to stand with α-SnP for 4 days at 25 °C. [c] The compound was absorbed from the vapor phase at 60 °C.

Table II. X-ray Powder Data for $Sn(C_5H_5N)_{0.41}(HPO_4)_2 \cdot H_2O$[a]

hkl	d_{obsd}, Å	d_{calcd}, Å	I
002	11.48	11.49	VVS
004	5.74	5.75	VS
110	4.23	4.24	M
200	4.04	4.04	M
006	3.82	3.82	M
202	3.42	3.46	W
108	3.08	3.06	M
302	2.85	2.85	VW
020	2.49	2.49	S
220	2.11	2.11	VW
400	2.02	2.02	VW
$\bar{1}30$	1.63	1.63	VW
330	1.44	1.45	VW

[a] Lattice constants: a = 8.60 (5) Å, b = 4.98 (3) Å, c = 24.46 (10) Å, β = 110.0 (5)°. λ = 1.5418 Å.

Preparation of Intercalation Compounds. Ca. 0.25-g samples of tin(IV) hydrogen phosphate were placed in contact with pure liquid (pyridine, piperidine, aniline, *m*-toluidine, 3,5-dimethylaniline, formamide, and *N,N*-dimethylformamide) or with concentrated aqueous solutions (urea, thiourea and pyridine) at 25 °C for 4 days. Benzenic solutions were used in the cases of 2,2′-bipyridine, 4,4′-bipyridine, and pyridine, under the same conditions. Dimethyl sulfoxide vapors at 60 °C for 2 days were used for the intercalation process. The organic chemicals were either Ega-Chemie or Panreac reagents.

Characterization of the Products. X-ray films were obtained in Huber Debye–Scherrer cameras with diameters of 11.46 cm using a Siemens X-ray generator with nickel-filtered Cu Kα radiation. The powder X-ray diffraction patterns of the products can be indexed on a monoclinic cell with the a and b axes quite similar to those observed in α-SnP. The 110, 200, 020, 220, and 400 reflections of the original product have been maintained in the intercalates, and reflections due to other lattice planes were weak or absent. The values of the interlayer distances were thus calculated as a mean value of the first three orders of the reflection corresponding to the basal spacing. TG and DTA analyses were caried out wiht a Rigaku-Thermoflex thermoanalyzer, at a heating rate of 10° min^{-1}. Infrared data were obtained on a Beckman spectrophotometer using KBr disks. The guest molecule:α-SnP ratio could be determined because the complexes are relatively stable. The composition was calculated from N analysis and thermogravimetric loss curves.

Results and Discussion

Intercalation of Pyridine, 4,4′-Bipyridine, and Piperidine. Aromatic and cyclic amines can be intercalated within the layers of $Sn(HPO_4)_2 \cdot H_2O$ by allowing the phosphate to react with the pure liquid or with the aqueous or benzenic solutions of the amines (Table I). Pyridine forms an intercalate of composition $Sn(C_5H_5N)_{0.41}(HPO_4)_2 \cdot H_2O$. The interlayer distance of the complex is 11.48 Å; this involves a increase in basal spacing of 3.65 Å. The complex obtained from the aqueous or the benzenic solution presents the same composition and interlayer distance. The powder X-ray diffraction pattern of the intercalate (see Table II) can be indexed on a monoclinic unit cell with a = 8.60 (5) Å, b = 4.98 (3) Å, c = 24.46 (10) Å, and β = 110.0 (5)° (a = 8.61 (4) Å, b = 5.02 (3) Å, c = 16.74 (8) Å, and β = 110.2 (5)° for α-$Sn(HPO_4)_2 \cdot H_2O$). The absence of $hk0$ lines, where $h + k \neq 2n$, suggests the retention of the n glide plane of the phosphate. These data indicate that the layer structure has been preserved, while the c axis has expanded.

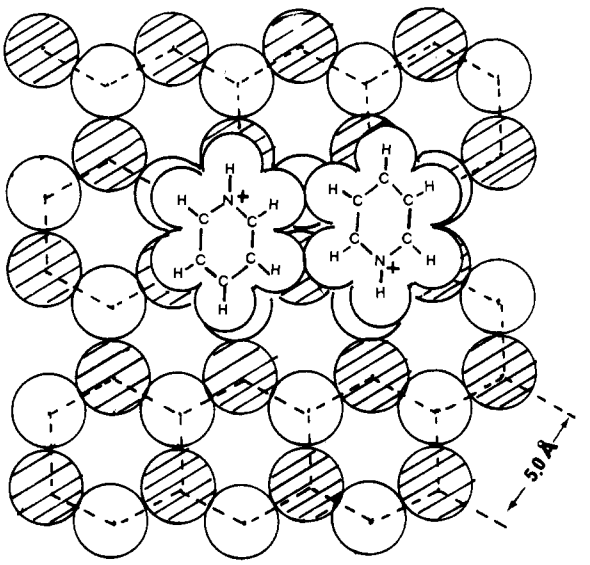

Figure 1. Idealized arrangement of the pyridinium ions in the interlayer region. Striped circles refer to –OH groups lying above, and open circles to those lying below, the intermediate plane.

When it is taken into account that the van der Waals thickness of the aromatic ring is 3.70 Å, the observed interlayer distance of the complex implies a parallel disposition of the pyridine ring to the layer. In the complex formation, pyridine is expected to act as a Brønsted base because of the α-SnP acidic hydrogen. Infrared data (ν(C–H) = 3090 cm^{-1}; $A_1$8a 1645, $B_1$9b 1550, $A_1$9b 1492, $B_2$4 750, $B_2$11 680 cm^{-1}) confirm the existence of pyridinium ions between the sheets of the phosphate.[10]

The found composition indicates that only about 20% of the available H atoms are saturated by the pyridine. This fact may be due to the parallel orientation of the aromatic ring within the interlayer space, which impedes total saturation of active sites. In Figure 1 it can be seen that the van der Waals area of two pyridinium ions[11] is almost equal to the free van der Waals area around 10 P–O–H groups, five in each layer. A similar stoichiometry in the complex of pyridine with α-$Zr(HPO_4)_2 \cdot H_2O$ was observed.[12] It has been suggested that this phenomenon may be due to the covering effect of the guest molecule. However, Hattori et al.[13] proposed that crystalline zirconium phosphate has two types of acid sites, each with remarkably different acid strength: a Lewis acid site, capable of accepting electrons, and a Brønsted acid site, capable of donating a proton. The strong-acid site is Brønsted type, and the ratio of weak acid to strong is much greater than unity. In this way, a weak base such as pyridine saturates the Brønsted acid sites, adopting a parallel disposition to the layer; the covering effect prevents total saturation of acid sites.

4,4′-Bipyridine also forms a complex with α-SnP from benzenic solution. The found composition is $Sn(C_{10}H_{10}N_2)_{0.25}(HPO_4)_2 \cdot H_2O$, and the interlayer distance is 12.4 Å. The composition is a consequence of the covering effect of the guest molecule; that is, 4,4′-bipyridine, bonded to a O_3POH group, renders an adjacent site unavailable for bonding since this site is covered.

4,4′-Bipyridine does not have a planar structure. The pyridyl rings are rotated 45° due to the ortho effect; thus, the observed increase in basal spacing (4.6 Å) is greater than is found in the

(10) Farmer, V. C.; Mortland, M. M. *J. Chem. Soc. A* **1966**, 344.
(11) Schomaker, V.; Pauling, L. *J. Am. Chem. Soc.* **1939**, *61*, 1769.
(12) Yamanaka, S.; Horibe, Y.; Tanaka, M. *J. Inorg. Nucl. Chem.* **1976**, *38*, 323.
(13) Hattori, T.; Ishiguro, A.; Murakami, Y. *J. Inorg. Nucl. Chem.* **1978**, *40*, 1107.

Table III. X-ray Powder Data for $Sn(C_6H_7N)_2(HPO_4)_2 \cdot H_2O$[a]

hkl	d_{obsd}, Å	d_{calcd}, Å	I
002	19.07	19.09	VVS
004	9.53	9.54	VS
006	6.36	6.36	S
110	4.26	4.24	W
200	4.04	4.04	VVS
114	3.72	3.72	S
108	3.35	3.34	M
020	2.48	2.49	S
	2.21		VW
220	2.11	2.12	VW
400	2.02	2.02	VW
$\bar{1}30$	1.63	1.64	VW
330	1.44	1.46	VW

[a] Lattice constants: $a = 8.56$ (6) Å, $b = 5.06$ (4) Å, $c = 38.72$ (13) Å, $\beta = 98.5$ (5)°. $\lambda = 1.5418$ Å.

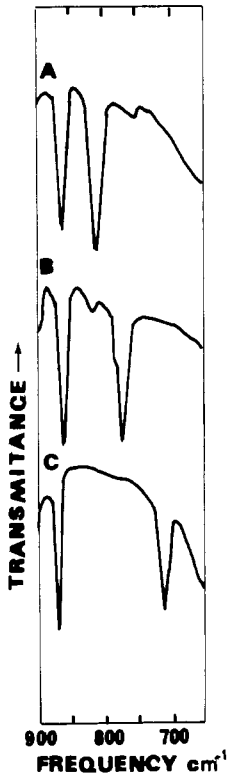

Figure 2. Infrared spectra of the complexes (A) aniline–α-SnP, (B) *m*-toluidine–α-SnP, and (C) 3,5-dimethylaniline–α-SnP.

pyridine complex. However, under the same conditions, 2,2′-bipyridine is not intercalated by α-SnP, probably because the lower basicity of the amine and steric hindrance prevent the intercalation.

Piperidine is also intercalated by α-SnP. The interlayer distance of the intercalate is 15.7 Å. The stoichiometry is $Sn(C_5H_{11}N)_{1.26}(HPO_4)_2 \cdot H_2O$; piperidine does not form stoichiometric compounds containing 2 ml of amine/mol of exchanger, because of the covering efect. This amine forms a bilayer of piperidinium ions between the sheets. The increase in basal spacing (7.9 Å) is greater than that observed in the piperidine–α-ZrP intercalate (5.8 Å).[14] DTA–TG analysis indicates the existence of one weakly bonded molecule of water, easily removed at 100 °C.

Intercalation of Aniline, *m*-Toluidine, and 3,5-Dimethylaniline. Generally, the substituted amines and some aromatic amines do not saturate all the α-SnP POH groups; However, aniline and derivatives can form stoichiometric intercalation compounds that contain 2 mol of amine/formula weight of α-SnP. The X-ray powder pattern of $Sn(C_6H_7N)_2(HPO_4)_2 \cdot H_2O$ was indexed with a monoclinic unit cell with lattice constants $a = 8.56$ (6) Å, $b = 5.06$ (4) Å, $c = 38.72$ (13) Å, and $\beta = 98.5$ (5)° and is given in Table III. The powder pattern is similar to those of the intercalates of *m*-toluidine and 3,5-dimethylaniline. The interlayer distances of the intercalates with aniline, *m*-toluidine, and 3,5-dimethylaniline are similar (~19 Å, see Table I). The observed increase in basal spacing of the aniline–α-SnP intercalate is higher than that observed in the α-SnP intercalate.[15] This may be explained if the higher α-SnP packing density is considered, which prevents an inclination of the intercalated molecule. Infrared spectra indicate that the amines are, in effect, ammonium ions between the layers of the phosphate. Figure 2 shows the infrared absorption peaks corresponding to the out-of-plane C–H bending vibrations of the aniline–α-SnP, *m*-toluidine–α-SnP, and 3,5-dimethylaniline–α-SnP complexes. The observed shift toward lower vibrational frequencies is due to the protonation of the amines.[16] DTA curves show endothermic peaks with temperatures higher than the boiling points of these amines. The stoichiometries of the aniline–α-SnP and *m*-toluidine–α-SnP intercalates are the same (2 mol of amine/mol of α-SnP). Nevertheless, the stoichiometry of the 3,5-dimethylaniline–α-SnP intercalate is lower because of the "covering effect" (1.4 mol of amine/mol of α-SnP).

Table IV. X-ray Powder Data for $Sn(C_3H_7NO)_{0.59}(HPO_4)_2 \cdot H_2O$[a]

hkl	d_{obsd}, Å	d_{calcd}, Å	I
002	13.31	13.30	VS
004	6.65	6.65	S
110	4.24	4.24	VS
200	4.04	4.07	M
202	3.77	3.77	VS
008/106	3.33	3.32	W
204	3.23	3.23	M
	2.74		VW
020	2.50	2.49	S
310	2.36	2.37	VW
220	2.12	2.12	VW
400	2.02	2.03	VW
$\bar{1}30$	1.63	1.63	VW
330	1.44	1.45	VW

[a] Lattice constants: $a = 8.71$ (6) Å, $b = 4.91$ (4) Å, $c = 27.42$ (12) Å, $\beta = 104.1$ (5)°. $\lambda = 1.5418$ Å.

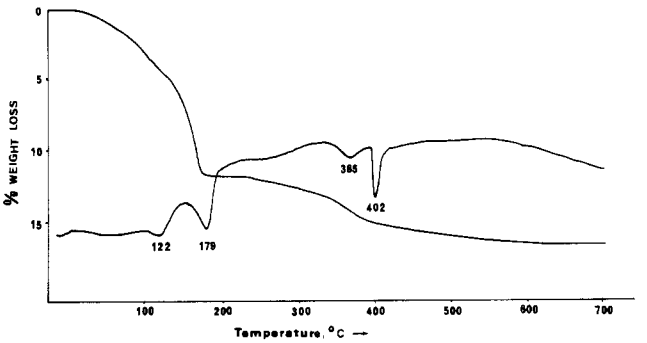

Figure 3. DTA–TG curves for the complex *N*,*N*-dimethylformamide–α-SnP.

Intercalation of *N*,*N*-Dimethylformamide. The intercalation of urea, thiurea, and formamide does not take place in concentrated aqueous solutions at 25 °C. However, a slightly more basic compound such as *N*,*N*-dimethylformamide is intercalated by α-SnP to form a complex with the stoichiometry $Sn(C_3H_7NO)_{0.59}(HPO_4)_2 \cdot H_2O$. The interlayer distance is 13.3 Å. This implies a increase in basal spacing of 5.5 Å. The observed increase suggests that *N*,*N*-dimethylformamide is perpendicular to the sheets. A similar increase was observed in the *N*,*N*-dimethylformamide–kaolinite complex, in which a perpendicular orientation

(14) Behrendt, D.; Beneke, K.; Lagaly, G. *Angew. Chem., Int. Ed. Engl.* **1976**, *15*, 544.

(15) Alberti, G.; Bernasconi, M. G.; Casciola. M.; Costantino, U.; Lucinani, M. L. XI Congrezo Nazionale di Chimica Inorganica, Arcavacata di Rende, Italy, 1978.

(16) Kross, R. D.; Fassel, V. A.; Murgoshes, M. *J. Am. Chem. Soc.* **1956**, *78*, 1332.

Table V. X-ray Powder Data for $Sn(C_2H_6OS)(HPO_4)_2 \cdot H_2O$[a]

hkl	d_{obsd}, Å	d_{calcd}, Å	I
002	11.29	11.31	VS
004	5.65	5.66	M
110	4.24	4.24	W
200	4.04	4.04	M
006	3.72	3.72	VW
	3.06		VW
020	2.49	2.49	S
220	2.12	2.12	VW
400	2.02	2.02	VW
$\bar{1}30$	1.64	1.63	VW
330	1.44	1.45	VW

[a] Lattice constants: $a = 8.62$ (5) Å, $b = 5.02$ (4) Å, $c = 24.16$ (10) Å, $\beta = 110.5$ (5)°. $\lambda = 1.5418$ Å.

of the amide was proposed.[17] The X-ray powder diffraction pattern of $Sn(C_3H_7NO)_{0.59}(HPO_4)_2 \cdot H_2O$ was indexed with a monoclinic unit cell with $a = 8.71$ (6) Å, $b = 4.91$ (4) Å, $c = 27.42$ (12) Å, and $\beta = 104.1$ (5)° (see Table IV).

In the infrared spectra, the carbonyl vibrational band group is displaced toward lower frequencies. This displacement indicates that the sheet–amide bond is by the carbonylic oxygen.[18] In the thermogravimetric curve (Figure 3) three different stages can be seen. The DTA curve supports this mode of decomposition and gives four distinct endotherms. The first and the second correspond to the removal of the water of crystallization and the evolution of the amide, respectively. The third and fourth endotherms correspond to the condensation process of orthophosphate to pyrophosphate.

The increase in basal spacing (5.5 Å) is greater than in the *N,N*-dimethylformamide–α-ZrP complex, where the water molecule is replaced by the amide. However, the *N,N*-dimethylformamide–α-SnP intercalate retains the water molecule; its presence is confirmed by infrared and thermal analysis.

Intercalation of Dimethyl Sulfoxide. The intercalation of dimethyl sulfoxide (Me_2SO) occurs as a vapor at 60 °C. The powder X-ray diffraction pattern of the product (Table V) can be indexed on a monoclinic unit cell with lattice constants $a = 8.62$ (5) Å, $b = 5.02$ (4) Å, $c = 24.16$ (10) Å, and $\beta = 110.5$ (5)°. The complex interlayer distance is 11.3 Å. This means an increase in basal spacing of 3.5 Å. A similar increase of 3.2 Å was observed in the complex Me_2SO–α-ZrP.[14] The stoichiometry is $Sn(C_2H_6OS)(HPO_4)_2 \cdot H_2O$. These results indicate that Me_2SO forms a monolayer between the sheets. Behrendt et al.[14] show that, in the intercalation of Me_2SO by α-ZrP, the water molecule is replaced by the almost spherical guest molecule. In this case, α-ZrP was allowed to react with liquid Me_2SO for several days at 60–80 °C. Thermogravimetric and infrared data indicate that

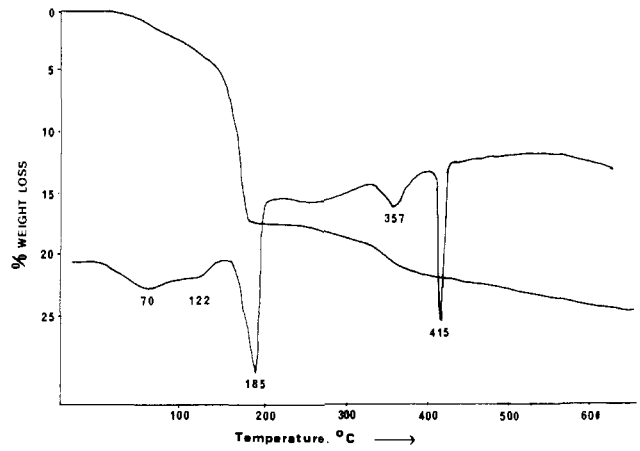

Figure 4. DTA–TG curves for the complex Me_2SO–α-SnP.

presence of water in the Me_2SO–α-SnP complex.

The observed infrared spectrum of Me_2SO intercalated into α-SnP is very similar to that seen in the Me_2SO–kaolinite complex.[19] ν(C–H) bands are displaced to higher frequencies (3020 and 2930 cm^{-1}). This displacement invalidates the theoretical concept of hydrogen bonding between the methyl group and the sheet. Me_2SO can bond to the α-SnP sheet through either the sulfur or the oxygen atoms. The infrared spectrum indicates that the latter mechanism is the more likely, if it is taken into account that the 720-cm^{-1} band is due to the asymmetric CS stretching and there is no symmetric CS vibration.

The DTA–TG curves show three different stages (Figure 4) corresponding to removal of the water of crystallization, the evolution of the sulfoxide, and the condensation of the hydrogen phosphate to give the pyrophosphate. The DTA peak at 185 °C corresponding to the Me_2SO evolution is very close to the boiling point of the organic molecule (190 °C). This implies that Me_2SO is weakly bonded to the sheet.

Acknowledgment. We thank the "Comision Asesora de Investigación Científica y Técnica" (Project 434/81) for financial support of the work carried out at the University of Málaga.

Registry No. $Sn(HPO_4)_2 \cdot H_2O$, 19513-14-5; α-SnP pyridine intercalate, 94979-03-0; α-SnP 4,4′-bipyridine intercalate, 94979-04-1; α-SnP piperidine intercalate, 94979-05-2; α-SnP aniline intercalate, 94979-06-3; α-SnP *m*-toluidine intercalate, 94979-07-4; α-SnP 3,5-dimethylaniline intercalate, 94979-08-5; α-SnP *N,N*-dimethylformamide intercalate, 94979-09-6; α-SnP dimethyl sulfoxide intercalate, 94979-10-9.

Supplementary Material Available: Listings of crystal data, details of preparation, and listings of X-ray powder diffraction patterns (9 pages). Ordering information is given on any current masthead page.

(17) Olejnik, S.; Posner, A. M.; Quirk, J. P. *Clay Miner.* **1970**, *8*, 421.
(18) Olejnik, S.; Posner, A. M.; Quirk, J. P. *Clays Clay Miner.* **1971**, *19*, 83.
(19) Olejnik, S.; Aylmore, L. A.; Posner, A. M.; Quirk, J. P. *J. Phys. Chem.* **1968**, *72*, 241.